Transverse momentum nonconservation at the ErAs/GaAs interface

K. J. Russell,* Ian Appelbaum,[†] and V. Narayanamurti

Gordon McKay Laboratory, Harvard University, Cambridge, Massachusetts 02138, USA

M. P. Hanson and A. C. Gossard

Materials Department, University of California, Santa Barbara, California 93106, USA

Because ErAs, a semimetal, grows epitaxially on GaAs(100), ErAs-base/ GaAs-collector metal-base transistors provide a uniquely simple system in which to study the interfacial transverse momentum conservation of hot electrons. This system is also of interest for metal-semiconductor superlattice thermal energy conversion devices that utilize ErAs as the interbarrier material. A key requirement for such devices to outperform bulk thermal energy converters is the nonconservation of transverse momentum. Our results, indicating total nonconservation of transverse momentum, could therefore lead to significantly more efficient thermal energy conversion devices.

In recent years, it has been proposed that superlattice structures can achieve thermoelectric power factors in excess of bulk values.[1,2] To attain such high efficiencies, these devices rely on transverse momentum nonconservation, which allows significantly more carriers to participate in the thermionic emission process.[2] Ballistic electron spectroscopy techniques provide one method of investigating transverse momentum conservation at a metal/semiconductor interface,[3,4] and in the current investigation these techniques are enhanced through the use of the band structure of the epitaxial ErAs films.[5–7]

Here we present results from a solid-state device version of ballistic electron emission microscopy/spectroscopy (BEEM/S).[3,4,8,9] These devices utilize an $\mathrm{Al/Al_2O_3/Al}$ tunnel junction for electron injection, and the results are averaged over the area of the device. Electrons emitted by the tunnel junction enter a metallic base, which they must traverse to enter a semiconductor collector [Fig. 1(a)]. The probability of entering the collector varies as the energy of the emitted electron is varied, allowing a spectroscopic characterization of the ErAs/GaAs interface. Since the oxide tunnel barrier thickness is fixed (and therefore the current-voltage relationship of the emitter is fixed), we normalize the collector current by dividing by the emitter current to extract base transport information. The semiconductor collector for all samples studied in this work is of the same structure: 100 nm GaAs n-type doped to 1×10^{17} cm^{-3} grown via molecular beam epitaxy (MBE) on (100) n-GaAs substrates. To form the base of the transistor, a film of ErAs of thickness d_{ErAs} is grown on the collector *in situ* and capped with 100 Å Al, also *in situ*. Four different samples were grown with varying ErAs film thickness: $d_{\mathrm{ErAs}}=120$, 138, 180, and 276 Å, ±5 Å, as measured by x-ray diffraction.

After collector and base fabrication, the sample is removed from the MBE system for further processing. $\mathrm{Al_2O_3}$ bonding pads 1000 Å thick are deposited using *e*-beam evaporation and shadow mask lithography. A native oxide of sufficient thickness forms on the exposed Al base layer during transport and processing, so no further oxidation is required to form the tunnel barrier. Two $\sim 100 \times 200 \ \mu\mathrm{m}^2$ Al emitters 1000 Å thick are thermally evaporated using shadow mask lithography such that they partially overlap the bonding pad (see Fig. 1), giving two tunnel junctions in parallel [Fig. 1(b)]. One of these junctions is shorted, creating an Ohmic contact to the base layer while leaving one junction as the emitter. Mesas are then wet etched down to the substrate to electrically isolate individual devices by submersion in 5% HCl for 10 s followed by 1 min submersion in $\mathrm{NH_4OH:H_2O_2:H_2O}$ $1:1:5$.

The devices are operated in common-base configuration at 80 K, and all measurements consist of varying the emitter voltage V_{eb} and measuring simultaneously the emitter current I_{eb} and the collector current I_{cb} at zero collector bias. Figure 2 shows a representative I_{cb}/I_{eb} trace taken on a device with $d_{\mathrm{ErAs}}=120$ Å. Decreasing V_{be} from zero bias raises the energy of electrons in the emitter with respect to those in the base, enabling them to couple to vacant states above the Fermi energy of the base. Because the probability of tunneling through the oxide barrier depends exponentially on the energy of the electron, the emitter current will be comprised mainly of electrons with energy near the Fermi energy of the emitter, which is eV_{be} above the Fermi energy of the base. This energetic resolution is what allows for the following spectroscopy. If the hot-electron mean-free-path of the base materials is assumed to be slowly varying for electron energies within a few electron volts of the Fermi energy, this technique can be used to estimate the Schottky barrier height E_{SB} at the base-collector interface. For $eV_{eb}<E_{SB}$, electrons have insufficient energy to overcome the Schottky barrier, and cannot enter the collector. The resulting I_{cb} has a small linear dependence on V_{eb} due to surface leakage problems associated with ErAs etching. This has been subtracted off in Fig. 2 for clarity but was left for the second derivative analysis since it gives no contribution. For $eV_{eb}>E_{SB}$, electrons can enter the collector, and I_{cb} increases superlinearly. Discerning this transition yields E_{SB}. As seen in Fig. 2, this measurement gives an estimate of 0.85 to 0.9 eV for the Schottky barrier of the $d_{\mathrm{ErAs}}=120$ Å sample. Similar results were obtained for $d_{\mathrm{ErAs}}=138$, 180, and 276 Å. These estimates agree with the theoretical prediction of 0.6 eV for the

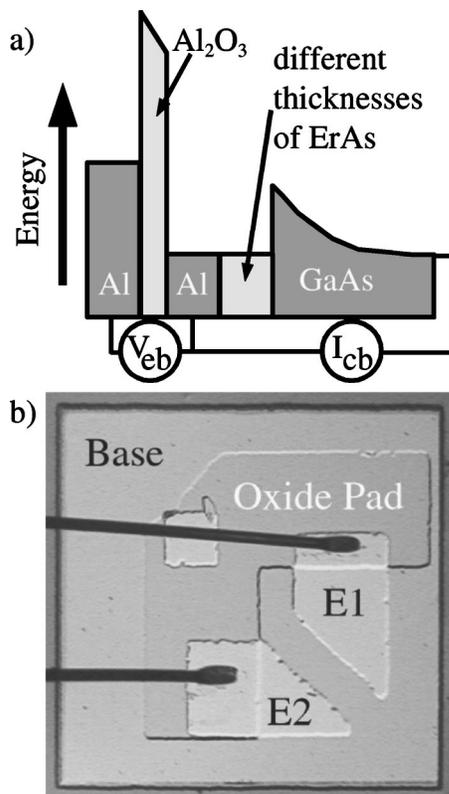FIG. 1. (a) Schematic conduction band diagram for an Al/ErAs metal-base transistor with nonzero emitter bias. Electrons tunnel across the Al_2O_3 barrier and enter the Al/ErAs base region at an energy approximately equal to eV_{eb}. For sufficient eV_{eb}, a fraction of electrons will traverse the base region and overcome the Schottky barrier to enter the GaAs collector. (b): Image of a working device. The Al/ErAs base is continuous across the mesa, and bonding wires contact each emitter (E1 and E2) above the Al_2O_3 bonding pad. One emitter is shorted to form an ohmic contact to the Al/ErAs base.

valence band barrier of a ErAs/GaAs "chain barrier",[10] since 1.48 eV − 0.6 eV = 0.88 eV, where 1.48 eV is the band gap of GaAs at 80 K.

In GaAs(100), the Schottky barrier is equivalent to the energy barrier between the Fermi level and the Γ valley of
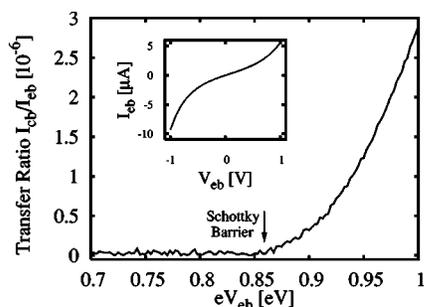

FIG. 2. Normalized transfer ratio I_{cb}/I_{eb} versus electron energy (eV_{eb}) is a simple method of estimating the Schottky barrier height for a given device. A representative trace from a 120 Å ErAs device shows a typical Schottky barrier height for these samples. (Inset): Typical emitter current-voltage trace displays characteristics of a single tunnel junction.
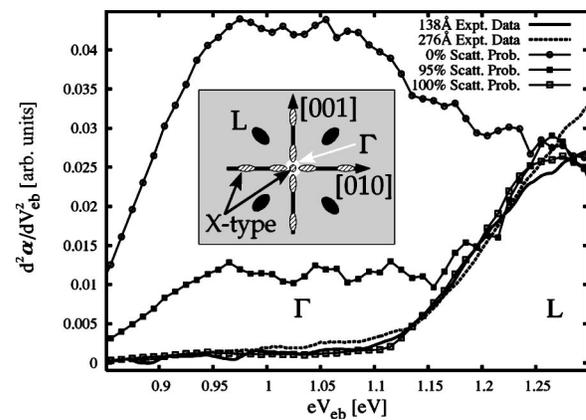

FIG. 3. Second derivative of the transfer ratio $\alpha = I_{cb}/I_{eb}$ with respect to the emitter energy provides a way of measuring relative contributions from different conduction valleys in the GaAs collector. Lines with symbols are simulation results; lines without symbols are experimental data. Second derivatives of the experimental results agree well with second derivative of the 100% interfacial scattering simulation. All traces are scaled to approximately coincide at 1.25 eV. Inset: Schematic diagram of the GaAs Brillouin zone and ErAs conduction valleys projected onto the interfacial plane. Electrons must scatter to reach states near an L point.

the conduction band at the base/collector interface. Other valleys, such as L and X, exist at higher energies, and these can be probed spectroscopically in the same manner as the Schottky barrier.[3,4,9] Since the energetic spacings of the conduction band valleys are bulk properties of GaAs, using spectroscopy to identify the thresholds of L and X does not reveal additional information about this particular system. However, because the Γ point is at the center of the Brillouin zone (see the inset of Fig. 3) and L is located at [111] (and symmetry-related points), spectroscopy above and below the L-valley threshold can reveal the degree of transverse momentum conservation of electrons crossing the ErAs/GaAs(100) interface.[11]

In a simple planar theory, the probability for tunneling is not dependent on the total energy of the electron, but on the amount of energy associated with momentum perpendicular to the metal/barrier interface.[12] This preferentially transmits Fermi energy electrons with a large perpendicular wave vector, and hence small transverse wave vector. As a result of the translational symmetry in the plane, this small transverse momentum is conserved as the electron tunnels into the base. Thus, the electron flux leaving the emitter is almost entirely directed perpendicular to the interface. Upon arriving at the base/collector interface, electrons with the proper energy and transverse momentum can enter available states in the conduction band of the collector. The Γ valley is at the center of the Brillouin zone and therefore is comprised of states with relatively little transverse momentum, while the L valley located at [111] (and symmetry-related points) consists of states with substantial transverse momentum. Therefore, although the Γ valley has a much lower density of states than the L valley,[13] the Γ valley can contribute a disproportionally large fraction of the collector current if the electron flux remains forward directed into the collector. A comparison of

contributions from the Γ and L conduction valleys can therefore indicate the extent to which transverse electron momentum is conserved while traversing the base and entering the collector.

A few objections have been raised against this simple theory. One is that the tunnel junction might not be perfectly planar, which would relax the transverse momentum conservation of the barrier and could result in a flux of electrons with larger spread in transverse wave vector.[14] Another is that the transport through the metal base layer is usually not well defined because it is typically a polycrystalline metal.[15,16] And finally, this theory does not account for multiple reflections within the base layer,[17] which would give the electrons more opportunities to scatter into states with a large transverse wave vector component. Initially, it appears that all three concerns apply in our case. The Al_2O_3 tunnel junction is formed on polycrystalline Al, and the lateral nonuniformity could result in an oxide barrier with local high-conductance areas and decreased translational symmetry. The nonepitaxial Al does not have well defined conduction channels, and there is an Al/ErAs interface also with poorly defined transport properties. Additionally, multiple reflections within the Al or ErAs or both could possibly lead to an increase in the transverse wave vector.

The key observation in our system is that the available states in ErAs within the relevant energy range (0.85 to 1.3 eV above the Fermi energy) are either near Γ or lie near planes containing Γ, X, and W (the {100} planes).[7] None of these states have a projection onto the GaAs L states in the plane of the interface, as can be seen in the inset of Fig. 3. The states with X-like character have symmetry-related states, some of which move more perpendicular to the interface and some which move more parallel. Those between Γ and X that are directed toward the interface will project directly onto Γ in the plane of the interface, while those between X and W may partially project onto Γ. This observation renders the above objections irrelevant because regardless of the electron's wave vector prior to entering the ErAs it will not have a [011] momentum component when it arrives at the ErAs/GaAs interface. It will have to scatter in order to enter the L valley in GaAs(100), and as a result we are able to analyze transverse momentum conservation specifically at that interface.

The validity of this analysis is critically dependent on our knowledge of the band structure of ErAs, which has not been widely studied. If we assume Ref. 7 to only be approximate, then we can at least conclude that some significant fraction of states will project onto Γ while none should project onto L. Ideally all relevant ErAs states would project onto Γ, since states which project onto neither Γ nor L cannot be collected without scattering. However, our second derivative analysis is very sensitive to deviations from 100% scattering, as will be shown below and in Fig. 3, so all that is necessary is for more than a few percent of ErAs states to project onto Γ and none onto L, which is the case. The contribution from ErAs states which do not project onto Γ decreases the resolution of our measurement, making it impossible to acertain the exact scattering probability of our system, especially if we were to obtain a probability less than 100%.

It is worth noting that BEEM/S studies have been done on epitaxial $CoSi_2$ (Refs. 18 and 19) and PtSi (Ref. 20) on Si.

Although these studies did not attempt to determine the degree of parallel momentum nonconservation, they illustrate the critical role played by the band structure of the epitaxial metal.

The system considered here can be modeled with a Monte Carlo simulation that treats interfacial scattering as an adjustable parameter and ignores multiple reflections as well as elastic scattering in the base.[21] Although the implementation is different, the theory is identical to that presented by Smith *et al.*,[11] with free-electron models describing the Al emitter and base, and an effective-mass model describing the GaAs collector. The ErAs band structure is effectively ignored because the tunneling process is expected to yield approximately the same distribution of transverse electron momenta, within the accuracy of published ErAs band structure information. Scattering is treated as S-wave in character, randomizing the total momentum of the electron. A tunnel barrier thickness of 15 Å and height of 2.2 eV (Ref. 22) were chosen to yield an emitter current density comparable to that obtained in our devices. The collector current was then normalized by the emitter current and the second voltage derivative was taken. As shown in Fig. 3, the probability of interfacial scattering greatly affects the relative magnitude of the second voltage derivatives at the Γ and L thresholds. As can be seen from the figure, the second voltage derivative of the normalized experimental data agrees well with the Monte Carlo simulation of 100% interfacial scattering, indicating complete nonconservation of transverse momentum at the ErAs/GaAs interface. The same conclusion can be reached by comparing the undifferentiated data, but in that case the correlation is less pronounced and the linear surface leakage current must be subtracted off. These results are consistent with the naive view that ErAs and GaAs have different crystal structures and therefore the interface lacks the translational symmetry necessary for conservation of transverse momentum. As a check on our reasoning, we can test for the effects of multiple reflections. The electron will arrive at the ErAs/GaAs interface within one of the available states regardless of the number of times it has traversed the base, so reducing the effect of reflections by increasing the ErAs film thickness should not have a significant impact on the spectroscopy. That this is the case is confirmed by noting the similarity in the second derivative spectroscopy from samples with $d_{ErAs}=138$ and 276 Å, as shown in Fig. 3.

One of the key points made by Vashaee and Shakouri[2] is the importance of transverse momentum nonconservation in heterostructure integrated thermionic (HIT) energy converters. Using a simulation of a HgCdTe superlattice structure, they compare the two extreme cases: perfect transverse momentum conservation and complete nonconservation. While the conserving system exhibited a maximum ZT of 1.25, the nonconserving system achieved a maximum ZT of over 3.25, illustrating the importance of transverse momentum nonconservation. Although the material system presented in this paper differs from that of Vashaee and Shakouri, their simulation demonstrates that the impact of transverse momentum nonconservation in the case of ErAs/GaAs could have significant implications for HIT energy converter design in GaAs-based materials, as well as III-V materials in general.

In conclusion, we have used an ErAs/metal-base hot-electron transistor structure to probe the interfacial character-

istics of epitaxial ErAs on GaAs(100). Using second derivative spectroscopy, we estimate 100% electron scattering probability at the ErAs/GaAs interface, indicating complete nonconservation of transverse momentum across the interface. The analysis leading to this estimate utilizes characteristics of the ErAs band structure, and the result is a simple system for the investigation of transverse momentum conservation. These findings could have dramatic implications for the future of solid state thermionics because transverse momentum nonconservation may lead to thermal energy conversion devices with significantly higher ZT values.

---

*Electronic address: krussell@deas.harvard.edu

†Present address: Electrical and Computer Engineering Department, University of Delaware, Newark, Delaware 19716.

[1] A. Shakouri, C. Labounty, P. Abraham, J. Piprek, and J. E. Bowers, in MRS Symposia Proceedings No. 545 (Materials Research Society, Pittsburgh, 1999), pp. 449–458.

[2] Daryoosh Vashaee and Ali Shakouri, Phys. Rev. Lett. **92**, 106103 (2004).

[3] V. Narayanamurti and M. Kozhevnikov, Phys. Rep. **349**, 447 (2001).

[4] J. Smoliner, D. Rakoczy, and M. Kast, Rep. Prog. Phys. **67**, 1863 (2004).

[5] C. J. Palmstrøm, N. Tabatabaie, and S. J. Allen, Appl. Phys. Lett. **53**, 2608 (1988).

[6] J. D. Ralston, H. Ennen, P. Wennekers, P. Hiesinger, N. Herres, J. Schneider, H. D. Muller, W. Rothemund, F. Fuchs, J. Schmalzin, and K. Thonke, J. Electron. Mater. **19**, 555 (1990).

[7] T. Komesu, H.-K. Jeong, J. Choi, C. N. Borca, P. A. Dowben, A. G. Petukhov, B. D. Schultz, and C. J. Palmstrøm, Phys. Rev. B **67**, 035104 (2003).

[8] W. J. Kaiser and L. D. Bell, Phys. Rev. Lett. **60**, 1406 (1988).

[9] L. D. Bell and W. J. Kaiser, Phys. Rev. Lett. **61**, 2368 (1988).

[10] A. G. Petukhov, B. T. Hemmelman, and W. R. L. Lambrecht, in Conference Proceedings of Microscopic Simulation of Inerfacial Phenomena in Solids and Liquids, 1998 (unpublished), p. 109.

[11] D. L. Smith, M. Kozhevnikov, E. Y. Lee, and V. Narayanamurti, Phys. Rev. B **61**, 13914 (2000).

[12] P. L. de Andres, F. J. Garcia-Vidal, K. Reuter, and F. Flores, Prog. Surf. Sci. **66**, 3 (2001).

[13] J. S. Blakemore, J. Appl. Phys. **53**, R123 (1982).

[14] I. Appelbaum, R. Sheth, I. Shalish, K. J. Russell, and V. Narayanamurti, Phys. Rev. B **67**, 155307 (2003).

[15] L. J. Schowalter and E. Y. Lee, Phys. Rev. B **43**, 9308 (1991).

[16] F. J. Garcia-Vidal, P. L. de Andres, and F. Flores, Phys. Rev. Lett. **76**, 807 (1996).

[17] L. D. Bell, J. Vac. Sci. Technol. A **15**, 1358 (1997).

[18] H. Sirringhaus, E. Y. Lee, and H. von Kanel, Phys. Rev. Lett. **73**, 577 (1994).

[19] K. Reuter, F. J. Garcia-Vidal, P. L. de Andres, F. Flores, and K. Heinz, Phys. Rev. Lett. **81**, 4963 (1998).

[20] Philipp Niedermann, Lidia Quattropani, Katalin Solt, Andrew D. Kent, and Øystein Fischer, J. Vac. Sci. Technol. B **10**, 580 (1992).

[21] Ian Appelbaum and V. Narayanamurti, Phys. Rev. B **71**, 045320 (2005).

[22] E. Cimpoiasu, S. K. Tolpygo, X. Liu, N. Simonian, J. E. Lukens, K. K. Likharev, R. F. Klie, and Y. Zhu, J. Appl. Phys. **96**, 1088 (2004).